Computing the polarimeter vector field of Λ_c^+ using its dominant hadronic mode

Remco de Boer[2], Mikhail Mikhasenko[1], Miriam Fritsch[2]
on behalf of the LHCb collaboration

[1] ORIGINS Excellence Cluster, Munich, Germany
[2] Ruhr University Bochum, Germany

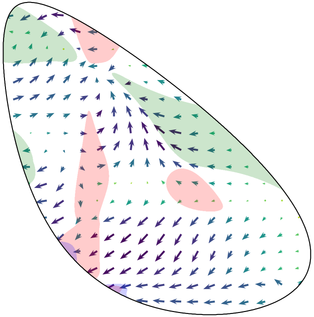

November 16th, 2022

4th Workshop on Future Directions in Spectroscopy Analysis,
Jefferson Lab

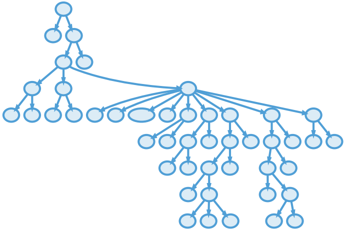

Overview

Two novelties from this study: **[LHCb-PAPER-2022-044]**

1. Aligned polarimeter vector field for $\Lambda_c^+ \to pK^-\pi^+$
2. Fast computations with symbolic amplitude models

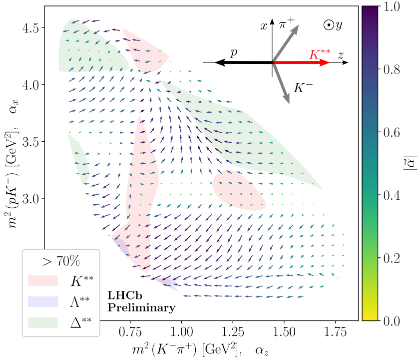

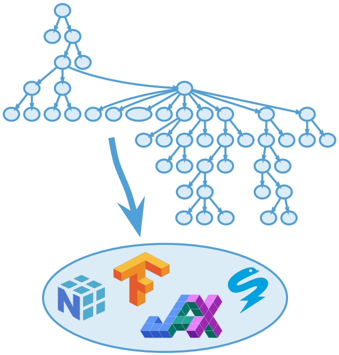

What can we learn by measuring polarization of hadrons?

Theory
Importance of polarization
Polarimetry
Implementation
Symbolic models
Self-documenting workflow
Data input
Cross-checks
Results
Polarimeter field
Uncertainties
Averaged polarimeter vector
Data availability
Summary

Polarization = preferred orientation of the spin of a particle in space

- Mechanism of quark hadronization [Brambilla:2010cs, Faccioli:2010kd, Butenschoen:2012px]
- BSM searches with $\Lambda_b^0 \to \Lambda_c^+ \ell^- \nu$
  [Konig:1993wz, Dutta:2015ueb, Shivashankara:2015cta, Li:2016pdv, Li:2016pdv, Datta:2017aue, Ray:2018hrx, DiSalvo:2018ngq, Penalva:2019rgt, Ferrillo:2019owd]
  E.g. sign of longitudinal polarization of Λ_c^+ provides a test for left-handedness of $b \to c$ current
- BSM searches with measurement of EDM with charmed mesons (SELDOM)
- Hadron spectroscopy, extending decay chains (next slide)
  - ✓ $\Lambda_b^0 \to J/\psi pK$ with $J/\psi \to \mu^+\mu^-$
  - ✓ $\mathfrak{B} \to J/\psi \overline{p} \Lambda$ with $\Lambda \to p\pi^-$
  - ? $\mathfrak{B}^+ \to \Lambda_c^+ \overline{\Lambda}_c^- K^+$ with $\Lambda_c^+ \to pK^-\pi^+$
  - ? $\Omega_b^- \to \Xi_c^+ \pi^- K^-$ with $\Xi_c^+ \to pK^-\pi^+$

Theory
Importance of polarization
Polarimetry
Implementation
Symbolic models
Self-documenting workflow
Data input
Cross-checks
Results
Polarimeter field
Uncertainties
Averaged polarimeter vector
Data availability
Summary

What can we learn by measuring polarization of hadrons?

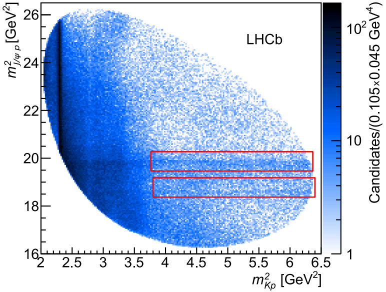

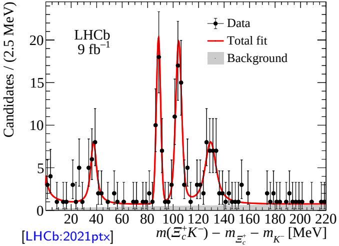

[LHCb:2021ptx]

Polarization determined from two-body final states

- $\Lambda_b^0 \to J/\psi(\to \mu^+\mu^-)pK^-$ [LHCb:2015yax]
  - Λ_b^0 is prompt (unpolarized)
  - 2D distribution is sensitive to P_c^+ spin
  - $J/\psi \to \mu^+\mu^-$ adds sensitivity for P_c^+ parity
- $\Xi_b^0 \to J/\psi(\to \mu^+\mu^-)p\Lambda(\to p\pi^-)$ [LHCb:2019aci]
  - P_{cs} in $J/\psi\Lambda^0$
  - $\Lambda^0 \to pK^-$ adds sensitivity to the P_{cs} spin

Hard to determine polarization, because three-body decay

- pentaquark searches: $\Lambda_b^0 \to \Lambda_c^+(\to pK^-\pi^+)\overline{D}^0K^-$
- heavy-baryon spectroscopy:
  $\mathfrak{B}_b \to \mathfrak{B}_c K\pi$ with $\mathfrak{B}_Q \in \{\Lambda_Q^+, \Sigma_Q^+, \Xi_Q^+, \Omega_Q^0\}$
  e.g. $\Omega_b^- \to \Xi_c^+ K^-\pi^-$ with $\Xi_c^+ \to pK^-\pi^+$ [LHCb:2021ptx]

Measuring polarization – two-body decays

Decay of a fermion is special – baryon in the final state averages angular distributions

Example: $\Lambda \to p\pi^-$

$$H_{\lambda_\Lambda,\lambda_p} = \langle p, \lambda_p; \pi^- | T_{\mathrm{weak}} | \Lambda, \lambda_\Lambda \rangle$$

$$\frac{2}{\Gamma}\frac{\mathrm{d}\Gamma}{\mathrm{d}\cos\theta} = 1 + P\alpha\cos\theta\,, \quad A_{FB} = \alpha P$$

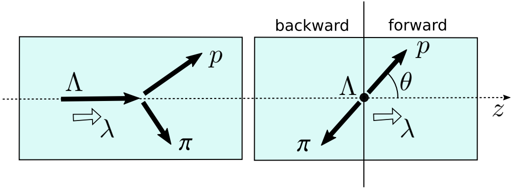

- $P = |\vec{P}|$ polarization, for $J = 1/2$, there are just tree d.o.f.
- α is the **asymmetry parameter** (analyzing power of the decay)

Appears only when both PV and PC

$$\alpha = \frac{|H_+|^2 - |H_-|^2}{|H_+|^2 + |H_-|^2} = -\frac{2\mathrm{Re}(H_S{}^* H_P)}{|H_S|^2 + |H_P|^2}$$

S-wave – parity violating (PV); P-wave – parity conserving (PC):

$$\Lambda\,(j^P = 1/2^+) \to p\,(j^P = 1/2^+)\,\pi^-(j^P = 0^-)$$

Theory
- Importance of polarization
- Polarimetry

Implementation
- Symbolic models
- Self-documenting workflow
- Data input
- Cross-checks

Results
- Polarimeter field
- Uncertainties
- Averaged polarimeter vector
- Data availability

Summary

Measuring polarization – two-body decays

Decay of a fermion is special – baryon in the final state averages angular distributions

Example: $\Lambda \to p\pi^-$

$$H_{\lambda_\Lambda,\lambda_p} = \langle p, \lambda_p; \pi^- | T_{\text{weak}} | \Lambda, \lambda_\Lambda \rangle$$

$$\frac{2}{\Gamma}\frac{\mathrm{d}\Gamma}{\mathrm{d}\cos\theta} = 1 + P\alpha\cos\theta, \qquad A_{FB} = \alpha P$$

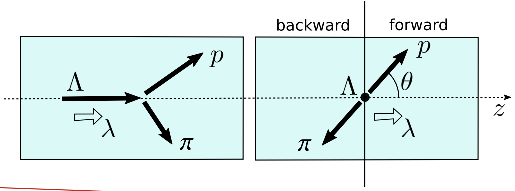

- $P = |\vec{P}|$ polarization, for $J = 1/2$, there are just tree d.o.f.
- α is the **asymmetry parameter** (analyzing power of the decay)

If we know α, we can measure P.

But what about **multibody** decays?

Appears only when both PV and PC

$$\alpha = \frac{|H_+|^2 - |H_-|^2}{|H_+|^2 + |H_-|^2} = -\frac{2\mathrm{Re}(H_S{}^* H_P)}{|H_S|^2 + |H_P|^2}$$

S-wave – parity violating (PV); P-wave – parity conserving (PC):

$$\Lambda\,(j^P = 1/2^+) \to p\,(j^P = 1/2^+)\,\pi^-(j^P = 0^-)$$

[Tsai:1971vv, Kuhn:1991cc, Davier:1992nw, Kuhn:1995nn, Kuhn:1982di, Kuhn:1993ra, Hagiwara:1989fn]

Theory
Importance of polarization
Polarimetry
Implementation
Symbolic models
Self-documenting workflow
Data input
Cross-checks
Results
Polarimeter field
Uncertainties
Averaged polarimeter vector
Data availability
Summary

Idea: similar relation for τ lepton decays,

$$\frac{\Phi}{\Gamma}\frac{\mathrm{d}\Gamma}{\mathrm{d}\Phi} \propto 1 + \vec{P}\cdot\vec{h}\,.$$

- $\vec{P}$ is a polarization of τ
- $\vec{h}$ is a **polarimeter vector**

Polarimeter vector of the τ lepton in the SM

- Direction depends on the final state, e.g.
  - for $\tau^- \to \pi^-\nu_\tau$ decay, $\vec{h} \uparrow\uparrow \vec{p}_{\pi^-}$
  - for $\tau^- \to \ell\nu_\tau\overline{\nu}_\ell$ decay, $\vec{h} \uparrow\uparrow \vec{p}_{\overline{\nu}_\ell}$
- Unit vector: $|\vec{h}| = 1$.

Measuring polarization – general multibody decays?

→ Dalitz-Plot Decomposition (DPD)

Factorization of variables describing dynamics and polarization [JPAC:2019ufm]:

$$T_{\nu_0,\{\lambda\}}(\phi,\theta,\chi;\tau) = \sum_{\nu} D^{1/2}_{\nu_0,\nu}(\phi,\theta,\chi)\, A_{\nu,\{\lambda\}}(\tau)$$

Polarization d.o.f.

- Euler angles in active ZYZ convention
- rotation of the system as rigid body
- polarization affects angular distribution

Dynamic d.o.f.

- Mandelstam variables of the subsystems
- describes resonances in the decay

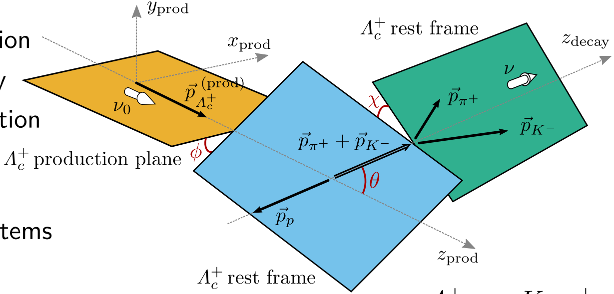

$\Lambda_c^+ \to pK^-\pi^+$

Model-agnostic representation of the decay rate

Using the SU(2) → SO(3) homomorphism, we get our polarized **master formula**,

$$|\mathcal{M}(\phi,\theta,\chi,\tau)|^2 = I_0(\tau)\left(1+\sum_{i,j=1}^{3} P_i R_{ij}(\phi,\theta,\chi)\alpha_j(\tau)\right),$$

where

- $I_0(\tau)$ is the unpolarized intensity
- $R(\phi,\theta,\chi) = R_Z(\phi)R_Y(\theta)R_Z(\chi)$ defines the decay plane orientation.
- $\alpha(\tau)$ is the **aligned polarimeter vector** field,

$$\vec{\alpha}(\tau) = \sum_{\nu',\nu,\{\lambda\}} A^*_{\nu',\{\lambda\}}\vec{\sigma}_{\nu',\nu}A_{\nu,\{\lambda\}} \Big/ I_0(\tau)\,.$$

It is specific for the decay, *does not depend on the production mechanism*.

Model-agnostic representation of the decay rate

Using the SU(2) → SO(3) homomorphism, we get our polarized **master formula**,

$$|\mathcal{M}(\phi,\theta,\chi,\tau)|^2 = I_0(\tau)\left(1+\sum_{i,j=1}^{3} P_i R_{ij}(\phi,\theta,\chi)\alpha_j(\tau)\right),$$

This study

where

- $I_0(\tau)$ is the unpolarized intensity
- $R(\phi,\theta,\chi) = R_Z(\phi)R_Y(\theta)R_Z(\chi)$ defines the decay plane orientation.
- $\alpha(\tau)$ is the **aligned polarimeter vector** field,

Determining polarization

1. provide $I_0(\tau)$ and $\vec{\alpha}(\tau)$
2. measure $|\mathcal{M}(\phi,\theta,\chi,\tau)|^2$
3. get $\vec{P}$ from fit

$$\vec{\alpha}(\tau) = \sum_{\nu',\nu,\{\lambda\}} A^*_{\nu',\{\lambda\}}\vec{\sigma}_{\nu',\nu}A_{\nu,\{\lambda\}} \Big/ I_0(\tau)\,.$$

It is specific for the decay, *does not depend on the production mechanism*.

Another application: extending amplitude models

Example: $B^+ \to \Lambda_c^+ \overline{\Lambda}_c^- K^+, \quad \Lambda_c \to pK\pi$

Normally, without polarization taken into account:

$$I\left(m^2_{\Lambda_c^+ K^+}, m^2_{\overline{\Lambda}_c^- K^+}\right) = \sum_{\nu_0,\bar{\nu}_0} \left| O^B_{\nu_0,\bar{\nu}_0}(m^2_{\Lambda_c^+ K^+}, m^2_{\overline{\Lambda}_c^- K^+}) \right|^2$$

Physics motivation

- exotic structures in $\Lambda_c^+ \overline{\Lambda}_c^-$
- studies of $\Xi_c{}^{**}$ in $\Lambda_c^+ K$

[BaBar:2007xtc, Belle:2017jrt, Belle:2018yob, LHCb:2022vns]

Another application: extending amplitude models

Example: $B^+ \to \Lambda_c^+ \bar{\Lambda}_c^- K^+$, $\quad \Lambda_c \to pK\pi$

Normally, without polarization taken into account:

$$I\left(m^2_{\Lambda_c^+ K^+}, m^2_{\bar{\Lambda}_c^- K^+}\right) = \sum_{\nu_0,\bar{\nu}_0} \left| O^B_{\nu_0,\bar{\nu}_0}(m^2_{\Lambda_c^+ K^+}, m^2_{\bar{\Lambda}_c^- K^+}) \right|^2$$

Polarimeter provides **10 additional degrees of freedom**:

$$I\left(m^2_{\Lambda_c^+ K^+}, m^2_{\bar{\Lambda}_c^- K^+}; \phi, \theta, \chi, m^2_{pK^-}, m^2_{K^-\pi^+}; \bar{\phi}, \bar{\theta}, \bar{\chi}, m^2_{\bar{p}K^+}, m^2_{K^+\pi^-}\right) =$$
$$\sum_{\nu_0,\bar{\nu}_0,\nu,\bar{\nu}} \sum_{\nu_0',\bar{\nu}_0',\nu',\bar{\nu}'} O^{B*}_{\nu_0',\bar{\nu}_0'}(m^2_{\Lambda_c^+ K^+}, m^2_{\bar{\Lambda}_c^- K^+}) O^B_{\nu_0,\bar{\nu}_0}(m^2_{\Lambda_c^+ K^+}, m^2_{\bar{\Lambda}_c^- K^+})$$
$$\times D^{1/2*}_{\nu_0',\nu'}(\phi,\theta,\chi) D^{1/2}_{\nu_0,\nu}(\phi,\theta,\chi) X^{\Lambda_c^+}_{\nu',\nu}(m^2_{pK^-}, m^2_{K^-\pi^+})$$
$$\times D^{1/2*}_{\bar{\nu}_0',\bar{\nu}'}(\bar{\phi},\bar{\theta},\bar{\chi}) D^{1/2}_{\bar{\nu}_0,\bar{\nu}}(\bar{\phi},\bar{\theta},\bar{\chi}) X^{\bar{\Lambda}_c^-}_{\bar{\nu}',\bar{\nu}}(m^2_{\bar{p}K^+}, m^2_{K^+\pi^-})$$

$$X_{\nu',\nu}(\tau) = \frac{I_0(\tau)}{2}\left(1 + \vec{\alpha}(\tau)\cdot\vec{\sigma}^P\right)_{\nu',\nu}$$

No need to fit these d.o.f.

Physics motivation

- exotic structures in $\Lambda_c^+ \bar{\Lambda}_c^-$
- studies of Ξ_c^{**} in $\Lambda_c^+ K$

[BaBar:2007xtc, Belle:2017jrt, Belle:2018yob, LHCb:2022vns]

Optional simplification: averaging over dynamic variables

Can the dynamic variables τ be integrated over, i.e disregarded in the analysis?

$$\frac{8\pi}{\Gamma}\frac{\mathrm{d}^3\Gamma}{\mathrm{d}\phi\,\mathrm{d}\cos\theta\,\mathrm{d}\chi} = 1 + \sum_{i,j=1}^{3} P_i R_{ij}(\phi,\theta,\chi)\overline{\alpha}_j\,,$$

where $\vec{\overline{\alpha}}$ is **averaged aligned polarimeter vector**.

Advantage / Disadvantage

+ Only need know three numbers in order to determine polarization.
− Uncertainty on $\vec{P}$ with averaged $\vec{\overline{\alpha}}$ is worse than with the full $\vec{\alpha}(\tau)$ field. [Davier:1992nw]

Analysis strategy

Strategy

- Implement $\Lambda_c^+ \to pK^-\pi^+$ models from [LHCb-PAPER-2022-002] with DPD
- Compute $\vec{\alpha}$ for every point of the $pK^-\pi^+$ Dalitz plot
- Propagate uncertainties of the angular analysis

Results

- Four distributions I_0, α_x, α_y, and α_z, computed on a grid of $m_{pK} \times m_{\pi K}$
- Statistical and systematic uncertainties for each grid point
- Averaged polarimeter vector values $\overline{\alpha}_x$, $\overline{\alpha}_y$, and $\overline{\alpha}_z$
- Proved loss of precision when using the averaged $\vec{\overline{\alpha}}$ vector
- Example of how to use these results, e.g. CPV properties of $\vec{\alpha}$

Implementation

Cross-check in two programming languages

Theory
Importance of polarization
Polarimetry
Implementation
Symbolic models
Self-documenting workflow
Data input
Cross-checks
Results
Polarimeter field
Uncertainties
Averaged polarimeter vector
Data availability
Summary

ComPWA
symbolic amplitude models

This analysis has been performed in two languages:

julia
ThreeBodyDecay.jl

python™
SymPy

Both implementations have been carefully documented on an interactive webpage

Next slides

A new technique: symbolic amplitude models

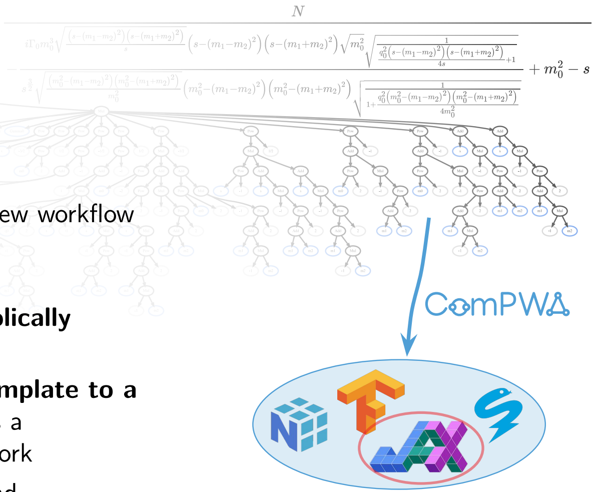

The Python implementation follows a new workflow that is facilitated by packages from the ComPWA Project (compwa-org.rtfd.io):

1. Formulate amplitude model **symbolically** with a Computer Algebra System
2. Use that symbolic expression as **template to a computational back-end**, such as a differentiable programming framework

We selected **JAX** as the fastest back-end

A new technique: symbolic amplitude models

Advantages of this workflow:

- Computational implementation is **outsourced to fast, optimized back-ends** from the Machine Learning and data science community
- Out-of-the-box GPU and multi-threading support
- Very easy to implement other parametrizations without having to worry about performance
- CAS simplifications result in performance boosts
- Symbolic amplitude models result in a **self-documenting workflow**

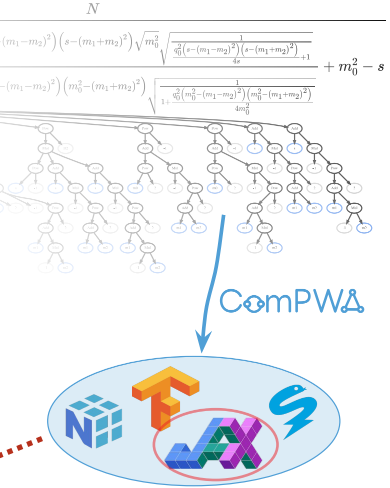

Works especially well for large computational models

Optional: **fit** with iminuit, SciPy, NLopt, ...

Living documentation

Maintaining reproducible and understandable analysis results

Self-documenting workflow
Our analysis results are automatically rendered as static webpages from Jupyter and Pluto notebooks:
lc2pkpi-polarimetry.docs.cern.ch
(CERN SSO until on arXiv)

The Python and Julia dependencies are pinned, so that the analysis is **fully reproducible** in around 2 hours

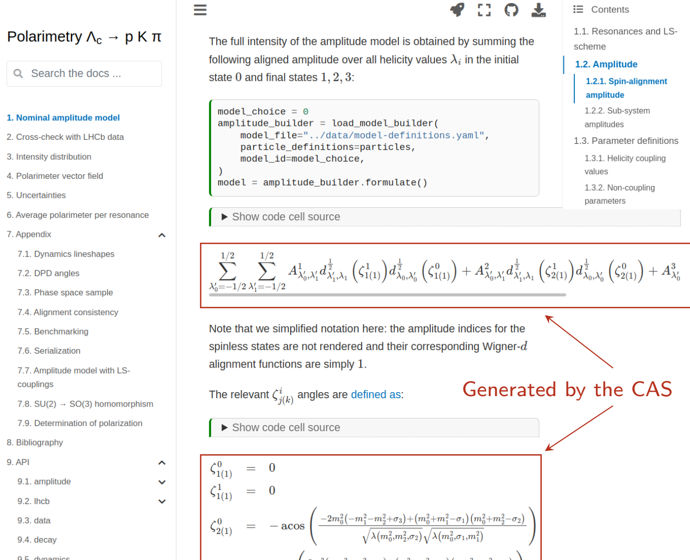

Polarimetry $\Lambda_c \to p\,K\,\pi$

Search the docs ...

1. Nominal amplitude model
2. Cross-check with LHCb data
3. Intensity distribution
4. Polarimeter vector field
5. Uncertainties
6. Average polarimeter per resonance
7. Appendix
7.1. Dynamics lineshapes
7.2. DPD angles
7.3. Phase space sample
7.4. Alignment consistency
7.5. Benchmarking
7.6. Serialization
7.7. Amplitude model with LS-couplings
7.8. SU(2) → SO(3) homomorphism
7.9. Determination of polarization
8. Bibliography
9. API
9.1. amplitude
9.2. lhcb
9.3. data
9.4. decay
9.5. dynamics

Contents

1.1. Resonances and LS-scheme
1.2. Amplitude
1.2.1. Spin-alignment amplitude
1.2.2. Sub-system amplitudes
1.3. Parameter definitions
1.3.1. Helicity coupling values
1.3.2. Non-coupling parameters

The full intensity of the amplitude model is obtained by summing the following aligned amplitude over all helicity values λ_i in the initial state 0 and final states $1, 2, 3$:

```
model_choice = 0
amplitude_builder = load_model_builder(
    model_file="../data/model-definitions.yaml",
    particle_definitions=particles,
    model_id=model_choice,
)
model = amplitude_builder.formulate()
```

▶ Show code cell source

$$\sum_{\lambda_0'=-1/2}^{1/2}\sum_{\lambda_1'=-1/2}^{1/2} A^1_{\lambda_0',\lambda_1'} d^{\frac{1}{2}}_{\lambda_1',\lambda_1}\left(\zeta^1_{1(1)}\right) d^{\frac{1}{2}}_{\lambda_0,\lambda_0'}\left(\zeta^0_{1(1)}\right) + A^2_{\lambda_0',\lambda_1'} d^{\frac{1}{2}}_{\lambda_1',\lambda_1}\left(\zeta^1_{2(1)}\right) d^{\frac{1}{2}}_{\lambda_0,\lambda_0'}\left(\zeta^0_{2(1)}\right) + A^3_{\lambda_0'}$$

Note that we simplified notation here: the amplitude indices for the spinless states are not rendered and their corresponding Wigner-d alignment functions are simply 1.

The relevant $\zeta^i_{j(k)}$ angles are defined as:

▶ Show code cell source

$$\zeta^0_{1(1)} = 0$$
$$\zeta^1_{1(1)} = 0$$
$$\zeta^0_{2(1)} = -\operatorname{acos}\left(\frac{-2m_0^2\left(-m_1^2-m_2^2+\sigma_3\right)+\left(m_0^2+m_1^2-\sigma_1\right)\left(m_0^2+m_2^2-\sigma_2\right)}{\sqrt{\lambda\left(m_0^2,m_2^2,\sigma_2\right)}\sqrt{\lambda\left(m_0^2,\sigma_1,m_1^2\right)}}\right)$$

Generated by the CAS

Input from LHCb

[LHCb-PAPER-2022-002] provides:

- a default amplitude model
- several alternative models with different dynamics parametrizations
- parameter values with error bars for each model

Present paper implements:

- default model and alternative models formulated with DPD [JPAC:2019ufm]
- helicity couplings have been remapped
- guaranteed identical dynamics lineshapes

Cross-checks

Visual comparison of the default amplitude model of [LHCb-PAPER-2022-002]

[LHCb-PAPER-2022-002]
(binned data)

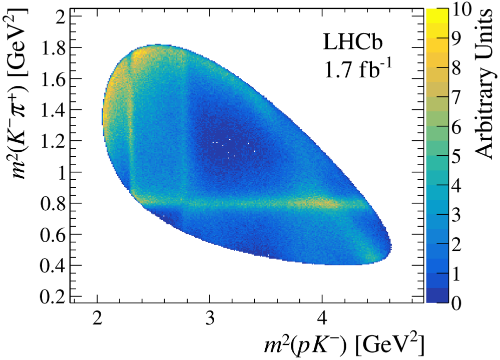

This analysis
(model evaluated on each Dalitz point)

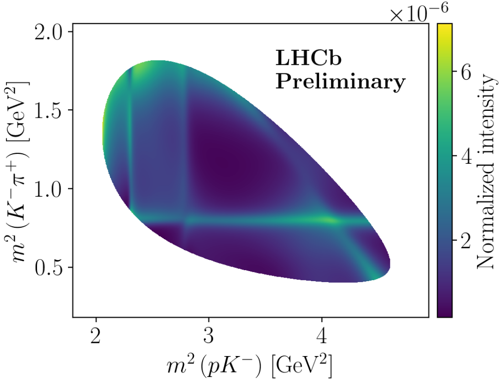

Cross-checks

Numerical test using code from LHCb-PAPER-2022-002

- Comparison for a single point in phase space
  - resonance lineshapes,
  - helicity amplitude per resonance
- Absolute differences at most 0.01%.

	Computed	Expected	Difference
ArD(1232)1	$\mathcal{H}^{\text{production}}_{D(1232),-\frac{1}{2},0}$		
A++	-0.488498+0.517710j	-0.488498+0.517710j	3.11e-14
A+-	0.894898-0.948412j	0.894898-0.948412j	7.61e-15
A-+	0.121490-0.128755j	0.121490-0.128755j	1.80e-14
A--	-0.222563+0.235872j	-0.222563+0.235872j	6.14e-15
ArD(1232)2	$\mathcal{H}^{\text{production}}_{D(1232),\frac{1}{2},0}$		
A++	-0.222563+0.235872j	-0.222563+0.235872j	6.14e-15
A+-	-0.121490+0.128755j	-0.121490+0.128755j	1.80e-14
A-+	-0.894898+0.948412j	-0.894898+0.948412j	7.61e-15
A--	-0.488498+0.517710j	-0.488498+0.517710j	3.11e-14
ArD(1600)1	$\mathcal{H}^{\text{production}}_{D(1600),-\frac{1}{2},0}$		

Main analysis result

Aligned polarimeter vector field in Dalitz plot coordinates

$$\left|\mathcal{M}(\phi,\theta,\chi,\tau)\right|^2 = I_0(\tau)\left(1+\sum_{i,j=1}^{3} P_i R_{ij}(\phi,\theta,\chi)\alpha_j(\tau)\right)$$

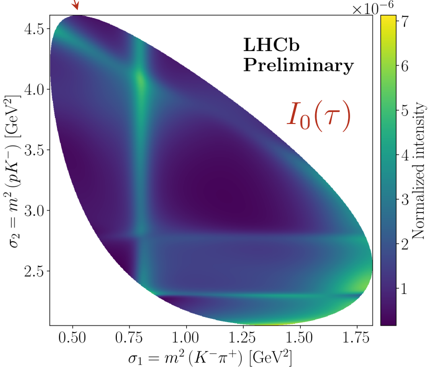

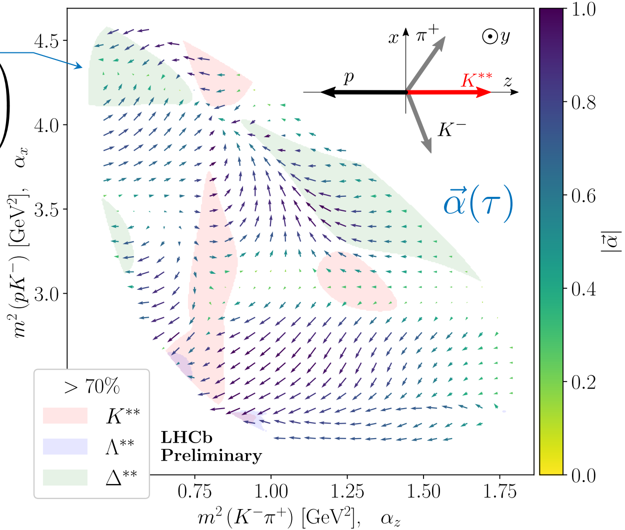

Understanding the polarimeter field

Example: $\Lambda_c^+ \to \Lambda(1520)\left(\to pK^-\right)\pi^+$

$\vec{\alpha}$ of individual contributions points in z-direction
when the resonance is aligned with z

Aligned

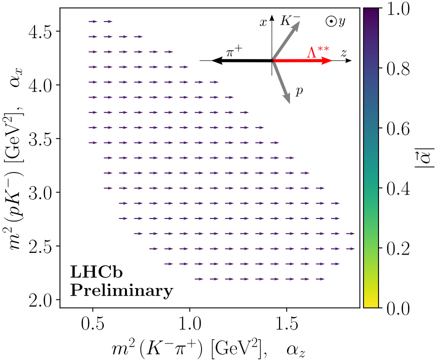

Misaligned

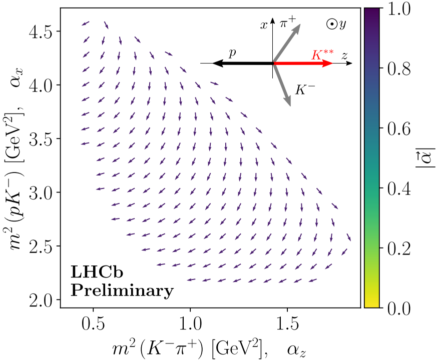

Propagation of uncertainties

Uncertainties over the polarimeter field have two components:

1. **Statistical + Systematic**:
   - parameter resampling of the default model using parameter error bars
   - parameter error bars include both stat. and syst. uncertainties, added in quadrature
   - take **RMS** over the resulting parameter-resampled distributions
2. **Model**:
   - determined from all alternative models
   - only central values of alternative models are considered
   - take **min-max** of the extrema

[LHCb-PAPER-2022-002, p. 19]

Table 8: Default amplitude model measured fit parameters describing the Λ contributions.

Parameter	Central Value	Stat. Unc.	Model Unc.	Syst. Unc.
$\mathrm{Re}\mathcal{H}^{\Lambda(1405)}_{1/2,0}$	-4.6	0.5	3.3	0.1
$\mathrm{Im}\mathcal{H}^{\Lambda(1405)}_{1/2,0}$	3.2	0.5	3.2	0.1
$\mathrm{Re}\mathcal{H}^{\Lambda(1405)}_{-1/2,0}$	10	1	12	0
$\mathrm{Im}\mathcal{H}^{\Lambda(1405)}_{-1/2,0}$	2.8	1.1	3.7	0.3
$\mathrm{Re}\mathcal{H}^{\Lambda(1520)}_{1/2,0}$	0.29	0.05	0.12	0.01
$\mathrm{Im}\mathcal{H}^{\Lambda(1520)}_{1/2,0}$	0.04	0.05	0.12	0.02
$\mathrm{Re}\mathcal{H}^{\Lambda(1520)}_{-1/2,0}$	-0.16	0.14	0.69	0.03
$\mathrm{Im}\mathcal{H}^{\Lambda(1520)}_{-1/2,0}$	1.5	0.1	1.3	0.0
$m^{\Lambda(1520)}$ [MeV]	1518.47	0.36	0.65	0.03
$\Gamma^{\Lambda(1520)}$ [MeV]	15.2	0.8	1.3	0.1
$\mathrm{Re}\mathcal{H}^{\Lambda(1600)}_{1/2,0}$	4.8	0.5	5.0	0.1
$\mathrm{Im}\mathcal{H}^{\Lambda(1600)}_{1/2,0}$	3.1	0.5	3.7	0.1
$\mathrm{Re}\mathcal{H}^{\Lambda(1600)}_{-1/2,0}$	-7.0	0.5	8.7	0.1
$\mathrm{Im}\mathcal{H}^{\Lambda(1600)}_{-1/2,0}$	0.8	0.6	2.0	0.2
$\mathrm{Re}\mathcal{H}^{\Lambda(1670)}_{1/2,0}$	-0.34	0.05	0.35	0.01
$\mathrm{Im}\mathcal{H}^{\Lambda(1670)}_{1/2,0}$	-0.14	0.05	0.22	0.02
$\mathrm{Re}\mathcal{H}^{\Lambda(1670)}_{-1/2,0}$	-0.57	0.10	0.46	0.02
$\mathrm{Im}\mathcal{H}^{\Lambda(1670)}_{-1/2,0}$	1.0	0.1	1.2	0.0
$\mathrm{Re}\mathcal{H}^{\Lambda(1690)}_{1/2,0}$	-0.39	0.10	0.23	0.02
$\mathrm{Im}\mathcal{H}^{\Lambda(1690)}_{1/2,0}$	-0.11	0.09	0.44	0.02
$\mathrm{Re}\mathcal{H}^{\Lambda(1690)}$	-2.7	0.2	2.4	0.0

Propagated uncertainties on the polarimeter field

Theory
Importance of polarization
Polarimetry
Implementation
Symbolic models
Self-documenting workflow
Data input
Cross-checks
Results
Polarimeter field
Uncertainties
Averaged polarimeter vector
Data availability
Summary

We compute $\vec{\alpha}^{(i)}(\tau)$ over a phase space sample, with i one of the parameter resamplings or one of the alterative amplitude models.

Uncertainties are then visualized separately, using

- **vector norm**: $\left|\vec{\alpha}^{(i)} - \vec{\alpha}^{\text{default}}\right|$
- **solid angle**:

$$\delta\Omega^{(i)} = \int_0^{2\pi}\int_0^{\theta} \mathrm{d}\phi\,\mathrm{d}\cos\theta = 2\pi\left(1-\cos\theta^{(i)}\right)$$

with $\cos\theta^{(i)} = \frac{\vec{\alpha}^{(i)}\cdot\vec{\alpha}^{\text{default}}}{|\vec{\alpha}^{(i)}||\vec{\alpha}^{\text{default}}|}$.

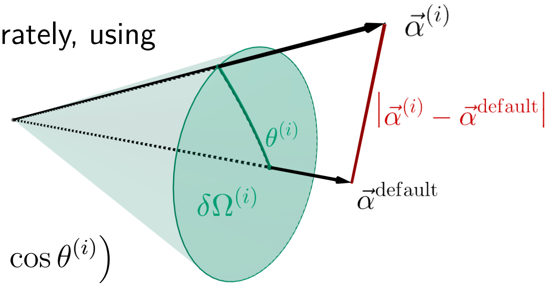

Propagated uncertainties on the polarimeter field

Theory
Importance of polarization
Polarimetry
Implementation
Symbolic models
Self-documenting workflow
Data input
Cross-checks
Results
Polarimeter field
Uncertainties
Averaged polarimeter vector
Data availability
Summary

vector norm

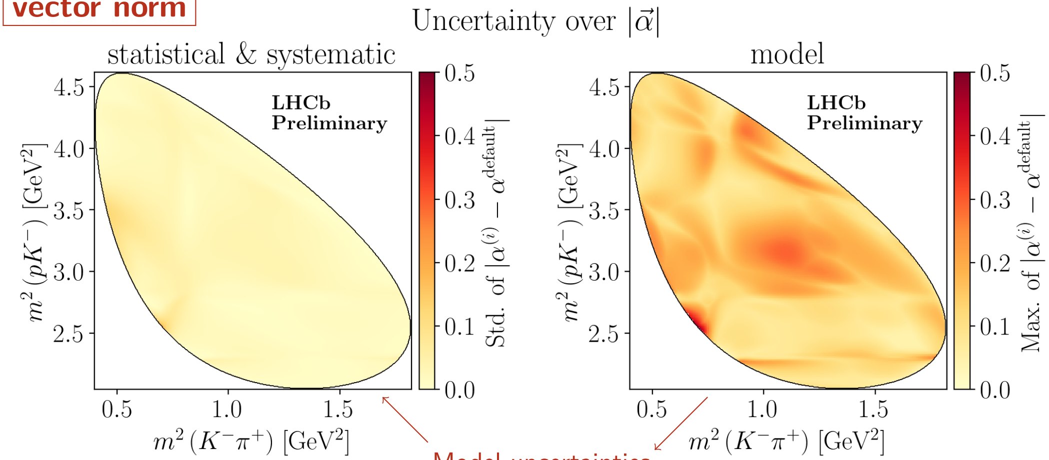

Model uncertainties dominate over stat.&syst.

Propagated uncertainties on the polarimeter field

solid angle

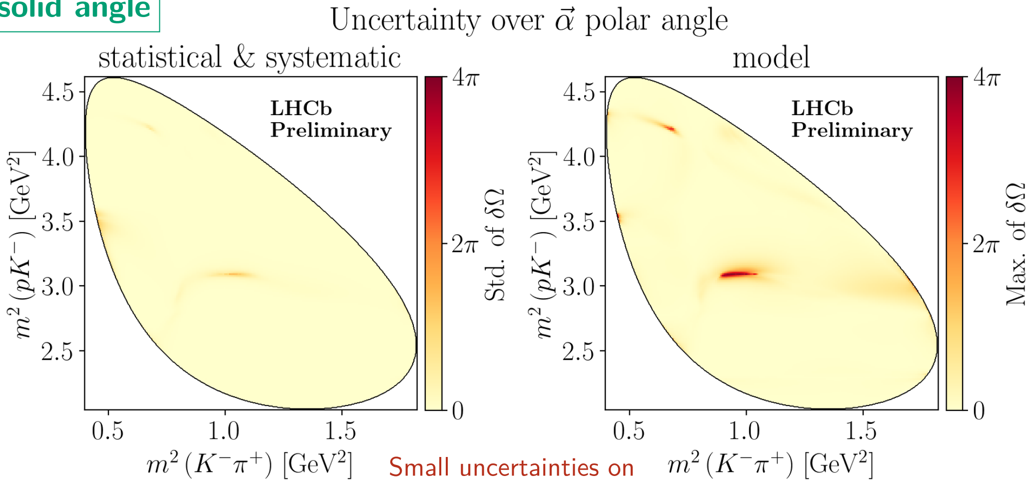

Small uncertainties on vector field directions

Averaged polarimeter vector

Polarimetry of $\Lambda_c \to pK\pi$

Remco de Boer

Theory
- Importance of polarization
- Polarimetry

Implementation
- Symbolic models
- Self-documenting workflow
- Data input
- Cross-checks

Results
- Polarimeter field
- Uncertainties
- Averaged polarimeter vector
- Data availability

Summary

Defining the averaged polarimeter vector as $\overline{\alpha}_j = \int I_0 \alpha_j \mathrm{d}^n\tau \,/\, \int I_0 \,\mathrm{d}^n\tau$, we get:

$$
\begin{aligned}
\overline{\alpha_x} &= \left(-62.6 \pm 4.5^{+8.4}_{-14.8}\right) \times 10^{-3}\,, \\
\overline{\alpha_y} &= \left(+8.9 \pm 8.9^{+9.1}_{-12.7}\right) \times 10^{-3}\,, && \text{(due to interference)} \\
\overline{\alpha_z} &= \left(-278.0 \pm 23.7^{+12.6}_{-40.4}\right) \times 10^{-3}\,, \\
\overline{|\alpha|} &= \left(669.4 \pm 9.3^{+15.3}_{-10.4}\right) \times 10^{-3}\,. && (\approx |\overline{\alpha}| \times 2.35)
\end{aligned}
$$

First uncertainty is stat.&syst (std.), second is model (extrema of alternative models).

Averaged polarimeter vector

Defining the averaged polarimeter vector as $\overline{\alpha}_j = \int I_0 \alpha_j \mathrm{d}^n\tau \;/\; \int I_0 \, \mathrm{d}^n\tau$, we get:

$$
\begin{aligned}
\overline{\alpha_x} &= \left(-62.6 \pm 4.5^{+8.4}_{-14.8}\right) \times 10^{-3}\,, \\
\overline{\alpha_y} &= \left(+8.9 \pm 8.9^{+9.1}_{-12.7}\right) \times 10^{-3}\,, \quad \text{(due to interference)} \\
\overline{\alpha_z} &= \left(-278.0 \pm 23.7^{+12.6}_{-40.4}\right) \times 10^{-3}\,, \\
\overline{|\alpha|} &= \left(669.4 \pm 9.3^{+15.3}_{-10.4}\right) \times 10^{-3}\,. \quad (\approx |\overline{\alpha}| \times 2.35)
\end{aligned}
$$

First uncertainty is stat.&syst (std.), second is model (extrema of alternative models).

Spherical coordinates (less correlated resampling uncertainty):

$$
\begin{aligned}
|\overline{\alpha}| &= \left(+285.1 \pm 24.0^{+37.9}_{-13.8}\right) \times 10^{-3}\,, \\
\theta\left(\overline{\alpha}\right) &= \left(+0.929 \pm 0.002^{+0.017}_{-0.011}\right) \times \pi\,, \quad \text{(small error!)} \\
\phi\left(\overline{\alpha}\right) &= \left(+0.955 \pm 0.045^{+0.067}_{-0.028}\right) \times \pi\,.
\end{aligned}
$$

Data availability

Justification of the 100x100 grid

$\vec{\alpha}(\tau)$ and $I_0(\tau)$ available in grid form:

- For propagating uncertainties:
  - grids for default model and for all alternative models
  - 100 parameter resamplings of the default model
- Grid size in $\delta m_{pK} \sim \Gamma_{\Lambda(1520)}$
- Toy fits of $\vec{P}$ with grids of **100x100**, 200x200, 500x500 $\Rightarrow$ negligible extra uncertainty

lc2pkpi-polarimetry.docs.cern.ch

averaged-polarimeter-vectors.json (33.7 kB)

polarimetry-field.json (67.9 MB)

polarimetry-field.tar.gz (26.2 MB)

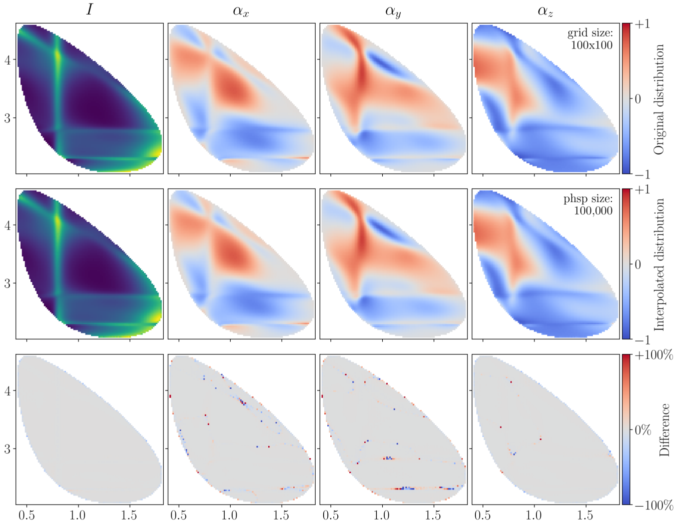

Summary

- **New result**: computed **polarimeter field for a three-body baryon decay** from recent $\Lambda_c^+ \to pK^-\pi^+$ amplitude analysis by LHCb
- The computed polarimeter field is offered for re-use in other analyses involving Λ_c
- **New approach**: **symbolic amplitude models** with JAX as computational back-end
- Extensive documentation on lc2pkpi-polarimetry.docs.cern.ch + analysis note show:
  - applications of the polarimeter grids
  - how to perform computations with symbolic amplitude models with the DPD formalism
- Computational workflow an be easily adapted to other channels

Theory
Importance of polarization
Polarimetry
Implementation
Symbolic models
Self-documenting workflow
Data input
Cross-checks
Results
Polarimeter field
Uncertainties
Averaged polarimeter vector
Data availability
Summary

Summary

- **New result**: computed **polarimeter field for a three-body baryon decay** from recent $\Lambda_c^+ \to pK^-\pi^+$ amplitude analysis by LHCb
- The computed polarimeter field is offered for re-use in other analyses involving Λ_c
- **New approach**: **symbolic amplitude models** with JAX as computational back-end
- Extensive documentation on lc2pkpi-polarimetry.docs.cern.ch + analysis note show:
  - applications of the polarimeter grids
  - how to perform computations with symbolic amplitude models with the DPD formalism
- Computational workflow an be easily adapted to other channels

Welcome to contact us for (1) applying the polarimeter fields or (2) trying computations with symbolic amplitude models!

Back-up slides

SU(2) → SO(3) homomorphism

Finding a general expression for $\vec{\alpha}(\tau)$

The **polarized decay rate** is given by:

$$\left|\mathcal{M}\right|^2 = \sum_{\nu_0,\nu_0',\{\lambda\}} \mathfrak{R}_{\nu_0',\nu_0} T^*_{\nu_0',\{\lambda\}} T_{\nu_0,\{\lambda\}}, \qquad \mathfrak{R}_{\nu_0',\nu_0} = \frac{1}{2}\left(1 + \vec{P}\cdot\vec{\sigma}^P\right)_{\nu_0',\nu_0}$$

$$T_{\nu_0,\{\lambda\}} = \sum_{\nu} D^{1/2}_{\nu_0,\nu}(\phi,\theta,\chi)\, A_{\nu,\{\lambda\}}$$

Trick for factoring out polarization [Cornwell:1997ke]

SU(2) is double cover of SO(3) spin $1/2$, 4π rotation

Explicit homomorphism with the non-trivial centre:

$$\phi : \mathrm{SU}(2) \to \mathrm{SO}(3), \qquad \phi(d) = R\,,$$

$$\phi(d) = \frac{1}{2}\mathrm{Tr}\left[D^{1/2*}(\phi,\theta,\chi)\sigma_i^P D^{1/2}(\phi,\theta,\chi)\sigma_j^P\right] = R_{ij}(\phi,\theta,\chi),$$

Appendix: $\vec{\alpha}$ for baryon + vector

Example: $\Lambda_c^+ \to K^{**}(\to \pi^+ K^-)p$ aligned to p

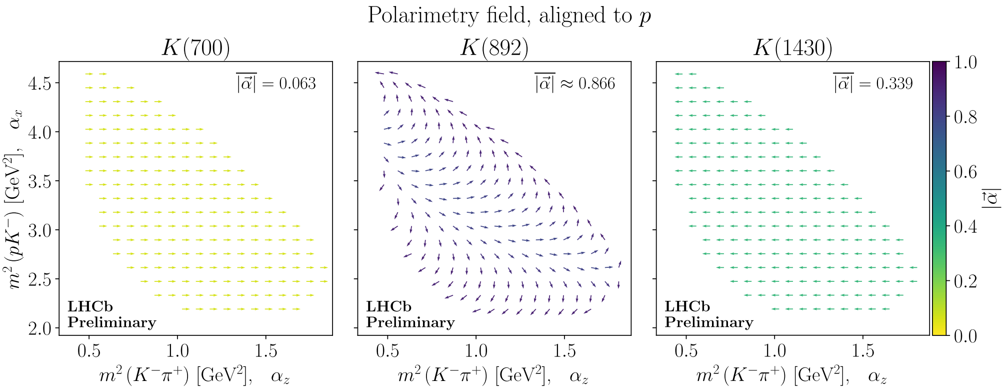

$1/2^\pm \to 1/2^+ \otimes 0^-$

$1/2^\pm \to 1/2^+ \otimes 1^-$

$1/2^\pm \to 1/2^- \otimes 0^-$

Intensity distributions are exactly the same for each DPD alignment

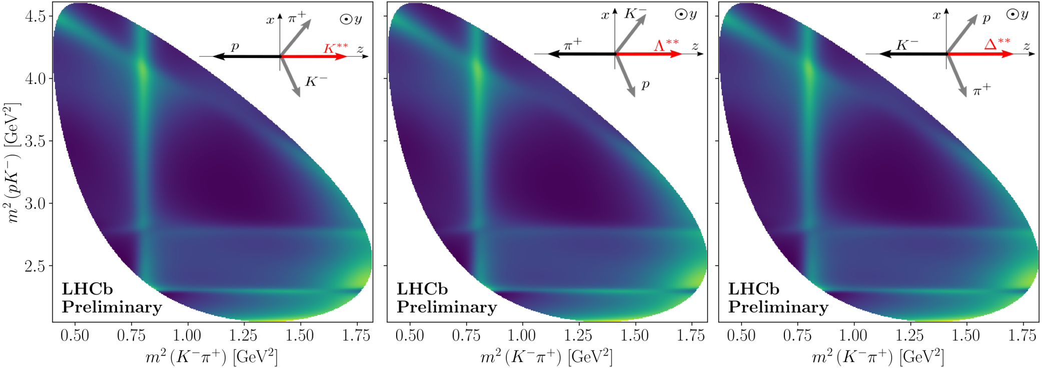

[Brambilla:2010cs] Brambilla *et al.*, "Heavy quarkonium: Progress, puzzles, and opportunities," *Eur. Phys. J. C*, vol. 71, no. 2, p. 1534, Feb. 2011, 10.1140/epjc/s10052-010-1534-9.

[Faccioli:2010kd] Faccioli *et al.*, "Towards the experimental clarification of quarkonium polarization," *Eur. Phys. J. C*, vol. 69, no. 3, pp. 657–673, Oct. 2010, 10.1140/epjc/s10052-010-1420-5.

[Butenschoen:2012px] Butenschoen and Kniehl, "J/ψ polarization at the Tevatron and the LHC: Nonrelativistic-QCD Factorization at the Crossroads," *Phys. Rev. Lett.*, vol. 108, no. 17, p. 172002, Apr. 2012, 10.1103/PhysRevLett.108.172002.

[Konig:1993wz] Konig *et al.*, "Determination of the $b \to c$ handedness using nonleptonic Λ_c decays," *Phys. Rev. D*, vol. 49, no. 5, pp. 2363–2368, Mar. 1994, 10.1103/PhysRevD.49.2363.

[Dutta:2015ueb] Dutta, "$\Lambda_b \to (\Lambda_c, p)\tau\nu$ decays within standard model and beyond," *Phys. Rev. D*, vol. 93, no. 5, p. 054003, Mar. 2016, 10.1103/PhysRevD.93.054003.

[Shivashankara:2015cta] Shivashankara *et al.*, "$\Lambda_b \to \Lambda_c \tau \bar{\nu}_\tau$ decay in the standard model and with new physics," *Phys. Rev. D*, vol. 91, no. 11, p. 115003, Jun. 2015, 10.1103/PhysRevD.91.115003.

[Li:2016pdv] Li *et al.*, "$\Lambda_c \to \Lambda_c \tau \bar{\nu}_\tau$ decay in scalar and vector leptoquark scenarios," *JHEP*, vol. 02, p. 068, Feb. 2017, 10.1007/JHEP02(2017)068.

[Datta:2017aue] Datta *et al.*, "Phenomenology of $\Lambda_b \to \Lambda_c \tau \bar{\nu}_\tau$ using lattice QCD calculations," *JHEP*, vol. 2017, no. 8, p. 131, Aug. 2017, 10.1007/JHEP08(2017)131.

[Ray:2018hrx] Ray *et al.*, "Probing new physics in semileptonic Λ_b decays," *Phys. Rev. D*, vol. 99, no. 1, p. 015015, Jan. 2019, 10.1103/PhysRevD.99.015015.

[DiSalvo:2018ngq] Di Salvo *et al.*, "Detailed study of the $\Lambda_b \to \Lambda_c \tau \bar{n} u_\tau$ decay," *Int. J. Mod. Phys. A*, vol. 33, no. 29, p. 1850169, Oct. 2018, 10.1142/S0217751X18501695.

[Penalva:2019rgt] Penalva *et al.*, "Further tests of lepton flavour universality from the charged lepton energy distribution in $b \to c$ semileptonic decays: The case of $\Lambda_b \to \Lambda_c \ell \bar{\nu} \ell$," *Phys. Rev. D*, vol. 100, no. 11, p. 113007, Dec. 2019, 10.1103/PhysRevD.100.113007.

[Ferrillo:2019owd] Ferrillo *et al.*, "Probing effects of new physics in $\Lambda_b^0 \to \Lambda_c^+ \mu^- \bar{\nu}_\mu$ decays," *JHEP*, vol. 2019, no. 12, p. 148, Dec. 2019, 10.1007/JHEP12(2019)148.

[LHCb:2015yax] LHCb Collaboration *et al.*, "Observation of $J/\psi p$ Resonances Consistent with Pentaquark States in $\Lambda_b^0 \to J/\psi K^- p$ Decays," *Phys. Rev. Lett.*, vol. 115, no. 7, p. 072001, Aug. 2015, 10.1103/PhysRevLett.115.072001.

[LHCb:2019aci] LHCb Collaboration *et al.*, "Isospin Amplitudes in $\Lambda_b^0 \to J/\psi \Lambda(\Sigma^0)$ and $\Sigma_b^0 \to J/\psi \Sigma^0(\Lambda)$ Decays," *Phys. Rev. Lett.*, vol. 124, no. 11, p. 111802, Mar. 2020, 10.1103/PhysRevLett.124.111802.

[LHCb:2021ptx] LHCb Collaboration *et al.*, "Observation of excited Ω_c^0 baryons in $\Omega_b^- \to \Xi_c^+ K^- \pi^-$ decays," *Phys. Rev. D*, vol. 104, no. 9, p. L091102, Nov. 2021, 10.1103/PhysRevD.104.L091102.

[Aiola:2020yam] Aiola *et al.*, "Progress towards the first measurement of charm baryon dipole moments," *Phys. Rev. D*, vol. 103, no. 7, p. 072003, Apr. 2021, 10.1103/PhysRevD.103.072003.

[Tsai:1971vv] Tsai, "Decay correlations of heavy leptons in $e^+e^- \to \ell^+\ell^-$," *Phys. Rev. D*, vol. 4, no. 9, pp. 2821–2837, Nov. 1971, 10.1103/PhysRevD.4.2821.

[Kuhn:1991cc] Kühn and Mirkes, "Angular distributions in semileptonic τ decays," *Phys. Lett. B*, vol. 286, no. 3, pp. 381–386, Jul. 1992, 10.1016/0370-2693(92)91791-7.

[Davier:1992nw] Davier *et al.*, "The optimal method for the measurement of tau polarization," *Phys. Lett. B*, vol. 306, no. 3-4, pp. 411–417, Jun. 1993, 10.1016/0370-2693(93)90101-M.

[Kuhn:1995nn] Kühn, "τ polarimetry with multimeson states," *Phys. Rev. D*, vol. 52, no. 5, pp. 3128–3129, Sep. 1995, 10.1103/PhysRevD.52.3128.

[Kuhn:1982di] Kühn and Wagner, "Semileptonic decays of the τ lepton," *Nucl. Phys. B*, vol. 236, no. 1, pp. 16–34, Apr. 1984, 10.1016/0550-3213(84)90522-4.

[Kuhn:1993ra] Kühn, "Tau kinematics from impact parameters," *Phys. Lett. B*, vol. 313, no. 3, pp. 458–460, Sep. 1993, 10.1016/0370-2693(93)90019-E.

[Hagiwara:1989fn] Hagiwara *et al.*, "τ polarization measurements at LEP and SLC," *Phys. Lett. B*, vol. 235, no. 1, pp. 198–202, Jan. 1990, 10.1016/0370-2693(90)90120-U.

[JPAC:2019ufm] Mikhasenko *et al.*, "Dalitz-plot decomposition for three-body decays," *Phys. Rev. D*, vol. 101, no. 3, p. 034033, Feb. 2020, 10.1103/PhysRevD.101.034033.

[BaBar:2007xtc] BaBar Collaboration *et al.*, "Study of $\bar{B}^- \to \Xi_c \bar{\Lambda}_c^-$ and $\bar{B}^- \to \Lambda_c^+ \bar{\Lambda}_c^- \bar{K}^-$ decays at *babar*," *Phys. Rev. D*, vol. 77, no. 3, p. 031101, Feb. 2008, 10.1103/PhysRevD.77.031101.

[Belle:2017jrt] Belle Collaboration *et al.*, "Observation of $\Xi_c(2930)^0$ and updated measurement of $B^- \to K^- \Lambda_c^+ \bar{\Lambda}_c^-$ at Belle," *Eur. Phys. J. C*, vol. 78, no. 3, p. 252, Mar. 2018, 10.1140/epjc/s10052-018-5720-5.

[Belle:2018yob] Belle Collaboration *et al.*, "Evidence of a structure in $\bar{K}^0\Lambda_c^+$ consistent with a charged $\Xi_c(2930)^+$, and updated measurement of $\bar{B}^0 \to \bar{K}^0 \Lambda_c^+ \bar{\Lambda}_c^-$ at Belle," *Eur. Phys. J. C*, vol. 78, no. 11, p. 928, Nov. 2018, 10.1140/epjc/s10052-018-6425-5.

[LHCb:2022vns] Collaboration, "Study of the $B^- \to \Lambda_c^+ \bar{\Lambda}_c^- K^-$," *Phys. Rev. D*, Nov. 2022, 10.48550/ARXIV.2211.00812.

[LHCb-PAPER-2022-002] LHCb Collaboration *et al.*, "Amplitude analysis of $\Lambda_c^+ \to pK^-\pi^+$ decays from semileptonic production," *Phys. Rev. D*, 2022, 10.48550/arXiv.2208.03262.

[Cornwell:1997ke] Cornwell, *Group Theory in Physics: An Introduction*. San Diego, CA: Academic Press, 1997. ISBN 978-0-12-189800-7